Nuclear Instruments and Methods in Physics Research B 566 (2025) 165798

Contents lists available at ScienceDirect

Nuclear Inst. and Methods in Physics Research, B

journal homepage: www.elsevier.com/locate/nimb

Full Length Article

Experimental study of production of nuclei heavier than ^{65}Cu in a copper target bombarded with 200 MeV/u ^{40}Ar ions

Edil Mustafin [a,*], Peter Katrik [a]

[a] GSI Helmholtzzentrum für Schwerionenforschung, Darmstadt, Germany

A B S T R A C T

This study examines the production and distribution of gamma-emitting nuclei heavier than ^{65}Cu in a copper target irradiated with a 200 MeV/u ^{40}Ar ion beam. Gamma spectra revealed that the gamma-emitting nuclei with mass numbers from 67 to 101 were concentrated near the range of the 40Ar ions. The centroids of nuclide distributions were observed to shift deeper with increasing mass, aligning with the reduced kinetic energy of the ^{40}Ar ions near the end of their path. These results demonstrate that the measured profiles of induced heavy-nuclide activity can be used to estimate projectile range in the target.

1. Introduction

The kinetic energy of a heavy ion beam penetrating a target decreases along the beam path due to the ionization losses. When the target is sufficiently thick, the beam particles lose all their kinetic energy and stop at a certain depth. This depth is called the projected ion range (shortly the range though this paper) and depends on the initial projectile energy. The majority of beam ions with the initial kinetic energy of a few hundred MeV/u reach the range without nuclear interaction with the target nuclei undergoing electronic stopping only. For example, only about 15 % of ^{40}Ar ions with a kinetic energy of 200 MeV/u experience a nuclear reaction with Cu nuclei along their path from the surface of the Cu target till the range (about 5 mm in this particular case). The nuclear interaction of ^{40}Ar with ^{63}Cu or ^{65}Cu (we consider a bulky Cu target with a natural mixture of isotopes with mass numbers 63 and 65 in this paper) mostly results in the fragmentation of Ar projectiles and Cu target nuclei [1]. However, synthesis of nuclei heavier than Ar and Cu is possible closer to the range of the beam. Some of them are gamma-emitters with lifetimes sufficiently long for their detection and identification after irradiation. In this paper, we report on the experimental observation of such products created in a bulky Cu target irradiated with a 200 MeV/u ^{40}Ar beam and show that the location of these nuclides gives a reasonable estimate of the ^{40}Ar range [2]. This work is a continuation of a series of activation studies conducted at GSI Helmholtzzentrum für Schwerionenforschung in Darmstadt over the past several years [1–14].

2. Experimental set-up

The Cu target was assembled in a stacked-foil geometry with square 10x10 cm foils of different thicknesses. The thicknesses of the foils are given in Table 1.

The total length of the target was 14 mm.

The ^{40}Ar beam was fast extracted from the SIS18 synchrotron of GSI-FAIR Darmstadt with a kinetic energy of 200 MeV/u. Before reaching the Cu target the beam passed through a 100 μm thick stainless steel vacuum window and a 69 cm long path in air. Calculations of ion stopping powers and ranges were performed using the ATIMA code [15] developed by GSI Helmholtz Centre for Heavy Ion Research, which provides accurate modeling of ion–matter interactions for heavy ions. According to ATIMA the residual range of the ^{40}Ar beam in the Cu target was about 5.15 mm, i.e. about in the foil #25.

The beam intensity was measured by a current transformer situated shortly upstream of the vacuum window. The uncertainty of the current measurement was about 3 %.

The irradiation lasted 2.5 h and the total number of ^{40}Ar ions delivered to the target was $3.86 \cdot 10^{13}$. The position and the size of the beam spot were detected by a 10 μm thick Pokalon organic foil attached to the target surface looking at the beam. The beam left a yellow spot on Pokalon. The spot was round in shape and about 1 cm in diameter.

The gamma spectra of each foil were measured separately after the "cooling-down" time by two different high-purity Ge detectors.

The first gamma detector had a larger crystal with the relative efficiency of about 75 % but it was available for acquisition for short time only (for about ten days). The energy gain was set relatively low and covered the broad energy range of gammas (from 40 keV up to 6 MeV). It

* Corresponding author.
E-mail address: e.mustafin@gsi.de (E. Mustafin).

https://doi.org/10.1016/j.nimb.2025.165798
Received 12 November 2024; Received in revised form 11 June 2025; Accepted 7 July 2025
Available online 17 July 2025

was used to detect and identify the gamma-emitters with lifetimes of a few days. As the larger detector was no longer available, the smaller one was used for the rest of the measurements. The second gamma detector had a smaller crystal and lower relative efficiency of about 20 % and was used to measure the spectra of gamma emitters with lifetimes of a few tens of days and longer. Its gain was set to cover the energy range of gammas from 40 keV up to 1.9 MeV. This provided more channels per gamma peak in the spectra.

Only one set of measurements done with the first detector is presented in this paper: the measurements were taken from about ten days of "cooling-down" after the end of irradiation (EoI) to about twenty days after the EoI. The acquisition time for different foils ranged from one hour to about half a day. The detector was calibrated for energy and efficiency values right before the start of the measurements.

Several sets of measurements were done with the second detector to measure the time evolution of the parent-daughter ratio for the couple $^{88}Zr \rightarrow {}^{88}Y$. The acquisition time for the long-living isotopes with low activity ranged from a day to a week for different foils. The second detector was calibrated several times between the series of measurements.

The energy calibration uncertainties were negligibly minor. The deviation of the peak centroids from the table energy values of the spectral lines was less than 0.5 keV in most cases. For both detectors, the uncertainties introduced by the efficiency calibration could be estimated to be about 5–6 % for the gamma lines with energies higher than 200 keV and could be about 10–15 % for the energy values around the 'knee'-value of 100 keV, i.e. from 40 keV to about 200 keV. The energy resolution was about FWHM = 2.1 keV and 1.9 keV at the 1332 keV line of ^{60}Co for the first and the second detectors respectively.

The gamma-ray spectrum analysis software GammaVision developed by ORTEC [16] was used for processing the gamma spectra. All the statistical uncertainties of the activity values in this paper were calculated based on the standard uncertainty calculation procedures of GammaVision.

Note, that the uncertainties of the intensity measurement by the current transformer and the uncertainties from the efficiency calibration of the detectors have a systematic origin and result in a coherent shift of the measured activity values for all foils. They do not affect the ratio of the activity values of any two foils to each other, i.e. they do not affect the shape of the activity depth profiles. Therefore, only the error bars from the statistical uncertainties calculated by GammaVision were taken into account for the measured activity values given in the pictures and tables further below.

It should be noted that the gamma-lines in the spectra were very dense, which did not allow for quantifying the activities for some nuclides that could be certainly recognised in the spectra. Especially it was difficult for the isobars. To demonstrate this, let us consider just one example. Let us compare the energies of gamma-lines for ^{67}Cu and ^{67}Ga (the corresponding abundances are given in the parenthesis):

^{67}Cu ($T_{1/2}$ = 61.83 h): 91.266 keV (7.0 %), 93.311 keV (16.1 %), 184.577 keV (48.7 %), 300.219 keV (0.797 %), 393.530 keV (0.22 %).

^{67}Ga($T_{1/2}$ = 3.2617 days): 91.265 keV (3.11 %), 93.310 keV (38.81 %), 184.576 keV (24.41 %), 300.217 keV (16.64 %), 393.527 keV (4.56 %).

One may notice that these nuclides have comparable lifetimes (i.e. no hope for separating them in time) and the energy lines are by far identical within the resolution of the measurement (FWHM was about 1.3 ÷ 1.4 keV for the region from 90 keV to 300 keV). The only difference is in the abundances. Fortunately, the 300 keV and 393.5 keV lines are represented almost purely by ^{67}Ga, because the abundances of ^{67}Cu at these lines are very low. Unfortunately, the 393.5 keV line was completely covered by the very intense 392.87 keV line of ^{88}Zr (abundance 97.29 %), thus the 300 keV line was the only available one to quantify the activity of ^{67}Ga. The difference in the intensities of the other ^{67}Ga lines (at 91 keV, 93 keV and 184 keV) allowed us to confirm the presence of ^{67}Cu gammas but it was not sufficient to quantify the activity of ^{67}Cu by subtracting the contribution of the ^{67}Ga. The 90 ÷ 200 keV lines are situated right around the 'knee' value of the efficiency calibration curve, where the efficiency calibration suffers from the highest uncertainties.

Further in the text, only the nuclides with reliably quantified activities are presented.

3. Results

The synthesis of the nuclides heavier than ^{40}Ar and Cu can be expected in the foils where the kinetic energy of the projectiles is sufficiently low to initiate the production of compound nuclei, that means at the end of the projectile path, which is in the vicinity of the projectile range. As mentioned above, according to ATIMA the residual range of the ^{40}Ar projectiles is about 5.15 mm, in the foils surrounding the foil #25. Indeed, the gamma-emitters heavier than Cu, namely, with mass numbers ranging from A = 67 (^{67}Ga) up to A = 101 (^{101}Rh) were detected in the foil #25 and the surrounding foils only. The activities given in Table 1 have less than 6 % uncertainties according to GammaVision. The values are given in Becquerels without normalizing by the number of delivered projectiles and by the foil thickness.

As mentioned in the previous section, not all the characteristic gamma lines of the identified nuclides were suitable for the quantification of the activities. The gamma lines used for activity calculation with the help of GammaVision are listed in Table 3 together with the corresponding abundances and half lives.

The EoI activities in Table 2 for heavier nuclides shift towards the foils with higher numbers. To quantify the value of the shift let us define the centroid of the activity depth distribution by the formula:

$$C(m)[mm] = \frac{5.075 \cdot A_{23} + 5.125 \cdot A_{24} + 5.175 \cdot A_{25} + 5.225 \cdot A_{26}}{A_{23} + A_{24} + A_{25} + A_{26}}$$

Table 2
The EoI activities (in Becquerels) for nuclides heavier than the target and projectile nuclei. The foil position is the middle of the foil.

Foil number	#23	#24	#25	#26
Foil position, mm	5.075	5.125	5.175	5.225
^{67}Ga	2300	5700	5500	720
^{71}As	0	3800	3000	0
^{72}As	0	12,200	8600	0
^{74}As	0	54	66	0
^{75}Se	0	66	80	0
^{79}Kr	0	3400	7900	0
^{83}Rb	0	0	206	0
^{83}Sr	0	2000	11,200	0
^{86}Zr	0	0	12,300	0
^{87}Y	0	360	6800	910
^{88}Zr	0	0	44	0
^{89}Zr	0	130	5300	1100
^{90}Nb	0	0	16,400	0
^{95}Tc	0	0	14,500	8800
^{97}Ru	0	0	320	200
^{100}Pd	0	0	2200	1800
^{100}Rh	0	0	7600	44,200
^{101m}Rh	0	0	550	620

Table 1
The thicknesses of the Cu foils.

Foil #	From #1 to #10	From #11 to #14	#15 and #16	#17 and #18	#19 and #20	#21	From #22 to #31	#32	From #33 to #40
Thickness, μm	50	100	500	1000	500	100	50	500	1000

Table 3
The characteristic gamma lines, used for the activity calculation, corresponding abundances and half lives of the identified nuclei.

Nuclide	Gamma line, keV	Abundance, %	Half live
^{67}Ga	300	16.64	61.83 h
^{71}As	175	81.75	65.30 h
^{72}As	834	81	26.0 h
^{74}As	596	59	17.77 days
^{75}Se	401	11.41	119.71 days
^{79}Kr	606	8.1	35.04 h
^{83}Rb	520	45	86.2 days
^{83}Sr	763	26.7	32.41 h
^{86}Zr	243	95.84	16.5 h
^{87}Y	485	89.8	79.8 h
^{88}Zr	393	97.3	83.4 days
^{89}Zr	909	99.04	78.41 h
^{90}Nb	1129	92.7	14.6 h
^{95}Tc	766	93.8	20.0 h
^{97}Ru	216	85.62	2.83 days
^{100}Pd	84	52	3.63 days
^{100}Rh	540	80.6	20.5 h
^{101m}Rh	307	81	4.34 days

Here $C(m)$ is the position of the centroid in *mm* for a given isotope with the mass number m, $A_{23}, A_{24}, A_{25}, A_{26}$ are the corresponding activities from Table 2 in the foils #23, #24, #25, #26 respectively. The dependence of $C(m)$ on the nuclide mass number is presented in Fig. 1.

The error bars in Fig. 1 were calculated by the standard error-propagation formula under the following assumptions:

- uncertainty of the foil positions are neglected;
- uncertainties for all measured activities is 6 % as calculated by Gamma Vision;
- there is no correlation between the measured activities in different foils.

Note that for four nuclides ^{83}Rb, ^{86}Zr, ^{88}Zr and ^{90}Nb, the error bars are zero because each of them has been found in one foil only, thus the centroids of their activities are assumed to be in the middle of the respective foil.

Although observed in the foils, ^{88}Y was not included in the list of nuclides in Table 2. ^{88}Y is the daughter product of ^{88}Zr. The time evolution of the ^{88}Zr and ^{88}Y activities is shown in Fig. 2.

The curves in Fig. 2 representing the time evolution of ^{88}Zr and ^{88}Y activities are determined by the least-square fit of the analytical solutions of the parent-daughter decay equations applied to ^{88}Zr as the parent nuclide and ^{88}Y as the daughter nuclide:

$$A_{Zr}(t) = A_{Zr}(0)exp(-\lambda_{Zr}t)$$

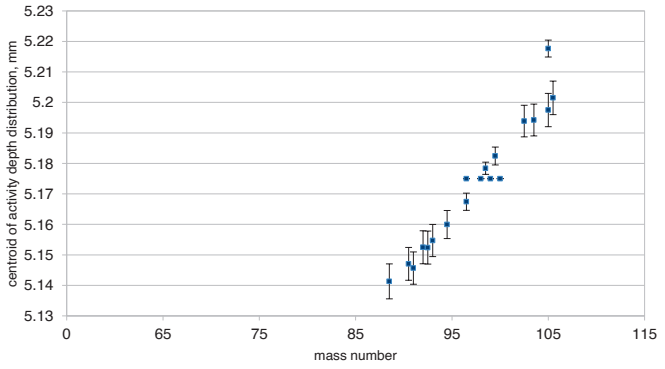

Fig. 1. The dependence of the centroid of the activity depth distribution $C(m)$ on the nuclide mass number.

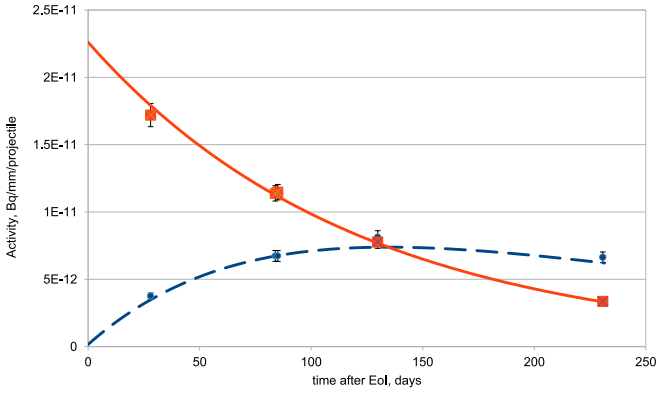

Fig. 2. Time evolution of ^{88}Zr and ^{88}Y activities in the foil #25. The the measured activities of ^{88}Y and ^{88}Zr are represented by the round and cross points respectively, the fit curves of ^{88}Y and ^{88}Zr activities are represented by the dashed and solid lines respectively.

$$A_Y(t) = A_{Zr}(0)[exp(-\lambda_{Zr}t) - exp(-\lambda_Y t)]\frac{\lambda_Y}{\lambda_Y - \lambda_{Zr}} + A_Y(0)exp(-\lambda_Y t)$$

to the set of the measured activities. Here $A_{Zr}(t)$ and $A_Y(t)$ are the activities of ^{88}Zr and ^{88}Y at time instant t, $A_{Zr}(0)$ and $A_Y(0)$ are their EoI activities and λ_{Zr} and λ_Y are their decay constants, respectively.

Extrapolation of ^{88}Y activity backward to EoI allows us to conclude that the activity of ^{88}Y was zero at EoI within the measurement uncertainties. Thus, it was not included in Table 2.

4. Discussion and conclusions

One may notice in Fig. 1 that there is an evident increase of $C(m)$ as the mass number of the induced nuclides increases. However, its span along the beam path is rather small: from about 5.14 mm to 5.22 mm. The residual range of ^{40}Ar in Cu calculated by ATIMA is 5.15 mm and the range straggling is about 0.01 mm. This means that according to ATIMA only a very few ^{40}Ar ions would be able to penetrate the Cu target as deep as 5.22 mm even when considering three standard deviations of the ^{40}Ar range distribution, i.e. 0.3 mm. The measurements show a considerable presence of those heavy products up to a depth of about 5.22 mm. The Cu target heating up during the irradiation and the corresponding decrease in its density along the beam path could be one of possible explanation for this discrepancy. Other possible sources of additional uncertainties could also be the inaccuracy in the foil thicknesses and energy losses in the vacuum window and the air.

The explanation of the mass-dependence of the centroid position seems to be obvious: the lower the collision energy of the projectile the heavier compound nuclei can be produced from ^{40}Ar + Cu reactions. To illustrate this, let us assume the range of ^{40}Ar was at 5.22 mm that corresponds to the centroid position of ^{100}Rh. Then for each centroid position from Fig. 2, we can get with the help of ATIMA the corresponding collision energy of ^{40}Ar projectiles. The result is presented in Table 4.

For example, the centroid position of ^{67}Ga activity is 74 μm upstream of the range of the projectile. According to ATIMA the kinetic energy of ^{40}Ar is 15.3 MeV/u at this distance from the range.

Another interesting fact is that the initial activity of ^{88}Y at EoI is zero. Only ^{88}Zr is present in the target when the activities are back-extrapolated to the EoI time instance. Moreover, ^{88}Zr should be itself (at least partially) the daughter product of the beta-decay of short-living proton-rich isobars. It means the nuclei synthesis products from the ^{40}Ar + Cu reactions were first born on the proton-rich side of the valley of stability on the nuclide chart and then experienced a sequence of beta-decays moving along the isobars towards the stable nuclei. Indeed, all the nuclides listed in Table 2 decay through either electron capture or

Table 4
The kinetic energy of ^{40}Ar at the depth corresponding to the activity centroid positions of nuclides with different mass numbers.

Nuclide	Distance of the activity centroid to the range, μm	Corresponding kinetic energy of ^{40}Ar, MeV/u
^{67}Ga	74	15.3
^{71}As	70	14.8
^{72}As	71	14.9
^{74}As	60	13.2
^{75}Se	62	13.5
^{79}Kr	57	12.7
^{83}Rb	42	10.1
^{83}Sr	46	10.9
^{86}Zr	46	10.9
^{87}Y	38	9.3
^{88}Zr	40	9.7
^{89}Zr	34	8.6
^{90}Nb	40	9.7
^{95}Tc	39	9.5
^{97}Ru	19	5.1
^{100}Pd	13	3.5
^{100}Rh	0	0
^{101m}Rh	17	4.8

positron emission, both resulting in the conversion of one proton into a neutron.

In conclusion, depth profiling of the gamma-active activation products with a mass number heavier than the mass number of the projectile and the target nuclei gives a reasonable estimate of the projectile range. In our particular case, the distribution span of such products was of the order of one foil thickness. Moreover, the centroid position of the heaviest gamma emitters provides the best range estimation.

Generally, the normalised activity per unit thickness of the nuclides heavier than Cu is of the same order of magnitude as the normalised activity per unit thickness of the nuclides lighter than Cu [1]. However, their integral activity is small compared to the integral activity of the nuclides lighter than Cu. The lighter nuclides are spread over the whole target thickness [1]. They provide the major contribution to the target activation, which is important for the radiation protection and component life-time activation studies. The heavier nuclides are concentrated in very narrow layers in the target close to the projectile range, which makes them suitable for determination/verification of the projectile range in the target.

CRediT authorship contribution statement

Edil Mustafin: Writing – review & editing, Writing – original draft, Validation, Supervision, Resources, Project administration, Methodology, Investigation, Formal analysis, Data curation, Conceptualization. **Peter Katrik:** Resources, Formal analysis, Data curation.

Declaration of competing interest

The authors declare that they have no known competing financial interests or personal relationships that could have appeared to influence the work reported in this paper.

Acknowledgments

The authors are grateful to E. Kozlova, A. Sokolov, and J. Hellmund for their time and effort in assisting with the gamma detectors, and would like to extend their deepest appreciation.

Data availability

Data will be made available on request.

References

[1] I. Strašík, E. Mustafin, M. Pavlovič, Residual activity induced by heavy ions and beam-loss criteria for heavy-ion accelerators, Phys. Rev. Specl. Topic. Accelerat. Beams 13 (2010).
[2] E. Mustafin, P. Katrík, M. Pavlovic, H. Weick, Depth-profiling of activity induced by 300 MeV/u 124Xe ions in aluminum: Ranges of heavy projectile fragments, Nucl. Inst. Methods Phys. Res. B 531 (2022) 82–92.
[3] P. Katrík, E. Mustafin, D.H. Hoffmann, M. Pavlovič, I. Strašík, Activation of accelerator construction materials by heavy ions, Nucl. Instrum. Method. Phys. Res. Sect. B - Beam Interact. Mater. Atoms 365 (2015) 525–528.
[4] P. Katrík, D.H.H. Hoffmann, E. Mustafin, I. Strašík, Experimental study of residual activity induced in aluminium targets irradiated by high-energy heavy-ion beams: A comparison of experimental data and FLUKA simulations, Matt. Radiat. Extrem. 4 (5) (1 September 2019).
[5] E. Mustafin, T. Seidl, A. Plotnikov, I. Strašík, M. Pavlovič, M. Miglierini, S. Stanček, A. Fertman, A. Lančok, Ion irradiation studies of construction materials for high-power acceleratorsradiat, Effect. Defect. Sol. 164 (7–8) (2009) 460–469.
[6] E. Mustafin, H. Iwase, E. Kozlova, D. Schardt, A. Fertman, A.V. Golubev, R. Hinca, M. Pavlovič, "Measured Residual Activity Induced by U Ions with Energy 500 MeV/u in Cu Target", Proceedings of EPAC2006 : 10th European Particle Accelerator Conference. Edinburgh, 26.-30.6.2006, 2006, 1834-1836.
[7] A. Fertman, E. Mustafin, R. Hinca, I. Strašík, M. Pavlovič, D. Schardt, N. Sobolevsky, A.V. Golubev, B. Sharkov, G. Fehrenbacher, I. Hofmann, H. Iwase, E. Kozlova, G. Mustafina, First results of an experimental study of the residual activity induced by high-energy uranium ions in steel and copper, Nucl. Instrum. Method. Phys. Res. Section B - Beam Interact. Mater. Atoms 60 (2007) 579–591.
[8] I. Strašík, E. Mustafin, A. Fertman, R. Hinca, M. Pavlovič, D. Schardt, N. Sobolevsky, A.V. Golubev, B. Sharkov, G. Fehrenbacher, I. Hofmann, H. Iwase, E. Kozlova, G. Mustafina, Experimental Study of the Residual activity Induced by 950 MeV/u Uranium Ions in Stainless Steel and copper, Nucl. Instrum. Method. Phys. Res. Sect. B - Beam Interact. Mater. Atom. 266 (2008) 3443–3452.
[9] I. Strašík, E. Mustafin, T. Seidl, M. Pavlovič, Experimental study and simulation of the residual activity induced by high-energy argon ions in copper, Nucl. Instrum. Method. Phys. Res. Sect. B - Beam Interact. Mater. Atom. (2010) 268573–268580.
[10] V. Chetvertkova, I. Strašík, A. Belousov, H. Iwase, N. Mokhov, E. Mustafin, L. Latysheva, M. Pavlovič, U. Ratzinger, N. Sobolevsky, Activation of aluminum by argon: Experimental study and simulations, Nucl. Instrum. Method. Phys. Res. Sect. B - Beam Interact. Mater. Atoms 269 (2011) 1336–1340.
[11] E. Kozlova, I. Strašík, A. Fertman, E. Mustafin, T. Radon, R. Hinca, M. Pavlovič, G. Fehrenbacher, H. Geissel, A.V. Golubev, H. Iwase, D. Schardt, Benchmark test of the fluka monte carlo code for residual production with 500 and 950 MeV/u uranium beams on copper and stainless steel targets, Nucl. Technol. 168 (2009) 747–751.
[12] I. Strašík, E. Kozlova, E. Mustafin, A. Smolyakov, N. Sobolevsky, L. Latysheva, M. Pavlovič, Simulation of the residual activity induced by high-energy heavy ions, Nucl. Technol. 168 (2009) 643–647.
[13] I. Strašík, V. Chetvertkova, E. Mustafin, M. Pavlovič, A. Belousov, Depth profiling of residual activity of 237U fragments as a range verification technique for 238U primary ion beam, Phys. Rev. Specl. Top. – Accelerat. Beams 15 (2012) 1–13, 071001.
[14] E. Mustafin, I. Hofmann, H. Weick, "Influence of electronic stopping power on the total neutron yield of energetic heavy ions", Nucl. Instrum. Meth. Phys. Res. Section A: Accelerat., Spectromet., Detect. Associat. Equipm., 501, (2–3) (1 April 2003) 553-558.
[15] Weick, H., Geissel, H., Iwasa, N., Scheidenberger, C., Rodriguez SANCHEZ, J.L., Prochazka, A., Purushotaman, S: Improved accuracy of the code ATIMA for energy loss of heavy ions in matter, In: GSI Scientific Report 2017, GSI Report 2018-1 (November 2018) 130-131, [energy-loss calculator available at https://www.isotopea.com/webatima].
[16] GammaVision Software, Version 6, ORTEC, Ametek Advanced Measurement Technology Inc., Oak Ridge, TN, USA.